IJISET - International Journal of Innovative Science, Engineering & Technology, Vol. 4 Issue 8, August 2017
ISSN (Online) 2348 – 7968 | Impact Factor (2016) – 5.264
www.ijiset.com

Heterojunction Devices And Its Application In Field Of Electronics

Tanmoy Biswas
Department of Computer Science, Syamaprasad College, 92, S P Mukherjee Road, Kolkata - 700026
tanmoybiswas.ece@gmail.Com

***Abstract*—**Review of various study conducted on Heterojunction device formed by thin film deposition of II-VI and III-V semiconductors over Silicon. Study includes voltage- current, capacitance- voltage characteristics, study of interface states, series resistance and effects of different elements on characteristics of thin films over Silicon. Heterojunction devices based on III-V and II-VI potential candidates for fabrication of efficient solar cells. Semiconductor diode lasers used in CD and DVD players and fibre optic transceivers are manufactured using alternating layers of various III-V and II-VI compound semiconductors to form lasing heterostructures. Heterojunction devices like Heterojunction bipolar junction transistor (HBT) and High electron mobility transistor (HEMT), heterostructures FET (HFET) or modulation-doped FET (MODFET has shown better high frequency and high power response than conventional Bipolar Junction Transistor. Investigating further into heterojunction may lead to fabrication of better devices and may also provide solution for fabrication of better photo voltaic cells for harnessing renewable energy sources.

Keywords: **Isotype, An-Isotype, SEM, STM, AFM,**

I. INTRODUCTION

A Heterojunction is formed between two dissimilar semiconductors. Usually two semiconductor with different bandgap and lattice constants are brought together to form a Heterojunction. Heterojunction forms a two-dimensional channel carrier at the interface with superior transport property. The superior transport property of Heterojunction has been widely exploited to make high-performance field-effect transistor. Heterojunction devices find its application in optical devices like semiconductor lasers.

II. BASICS OF HETEROJUNCTION

A semiconductor Heterojunction is formed by chemical bonding at the interface. Heterojunction is usually formed by the method of epitaxy and there forms a misfit between the two semiconductors. There are basically two types of heterojunction.

(a) Isotype heterojunction.
(b) Anisotype heterojunction.

Isotype heterojunction

When two semiconductors with similar conductivity having different bandgap and lattice constants are brought together, an Isotype heterojunction is formed. An Isotype heterojunction with two n-type semiconductors having bandgaps Eg_1 and Eg_2 has been shown in the figure(1.1). When the two semiconductors are brought together, band alignment takes place, which is as shown in the figure (1.2). The material that can be used is GaAs (Gallium Arsenide) as n type material with smaller bandgap and AlGaAs with larger bandgap (N type material).

Once the heterojunction is formed, electron transfer from AlGaAs to GaAs takes place since, the electron affinity is smaller in AlGaAs. This creates a depletion region in the AlGaAs and an accumulation region in the GaAs. Depending on the density of electrons transferred from AlGaAs to GaAs, forms a triangular potential well with lateral extent 100 – 150Å as shown in the figure (1.2).

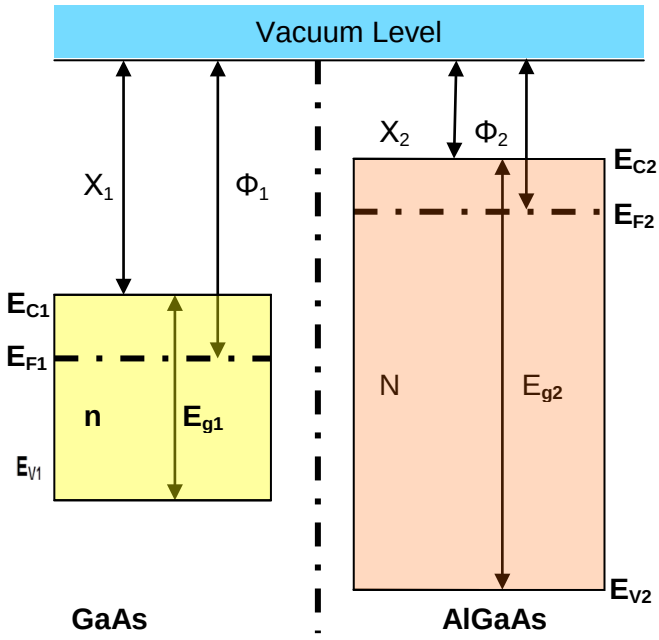

Figure (1.1), An Isotype heterojunction before formation.

IJISET - International Journal of Innovative Science, Engineering & Technology, Vol. 4 Issue 8, August 2017
ISSN (Online) 2348 – 7968 | Impact Factor (2016) – 5.264
www.ijiset.com

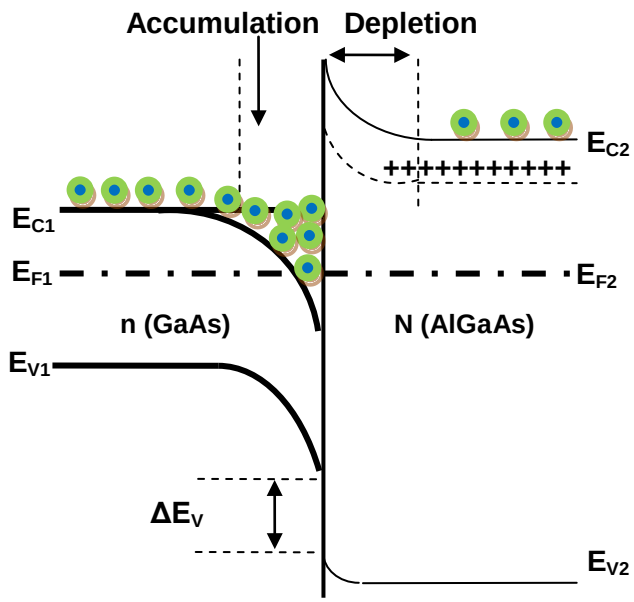

Figure (1.2), Transfer of electrons during accumulation and depletion layers.

Anisotype heterojunction

Two semiconductors with different conductivity form an Anisotype heterojunction. The P type semiconductor that has been used is of small energy bandgap with wide bandgap N type material. The band diagram of the individual semiconductors before they are fused to form heterojunction is shown in the figure (1.3).

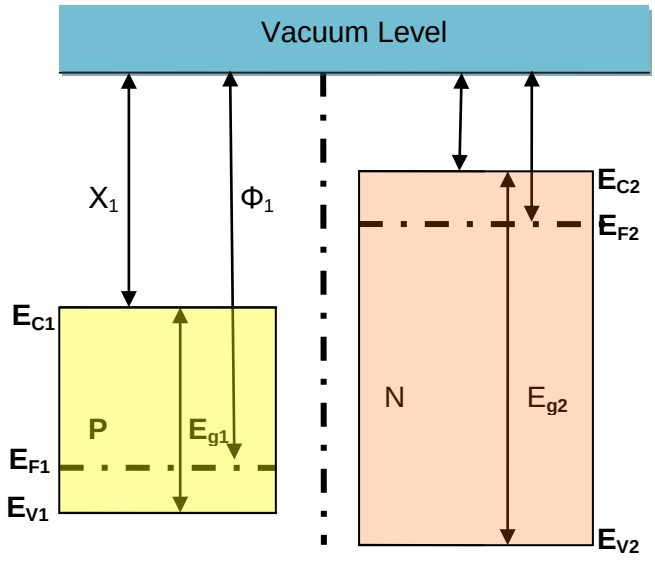

Figure (1.3), P and N type material energy band diagram before the junction formation.

The band diagram after junction formation has been shown in the figure (1.4).

Referring the figure (1.5), we have assumed P type semiconductor with narrow bandgap and N type material with wide band gap.

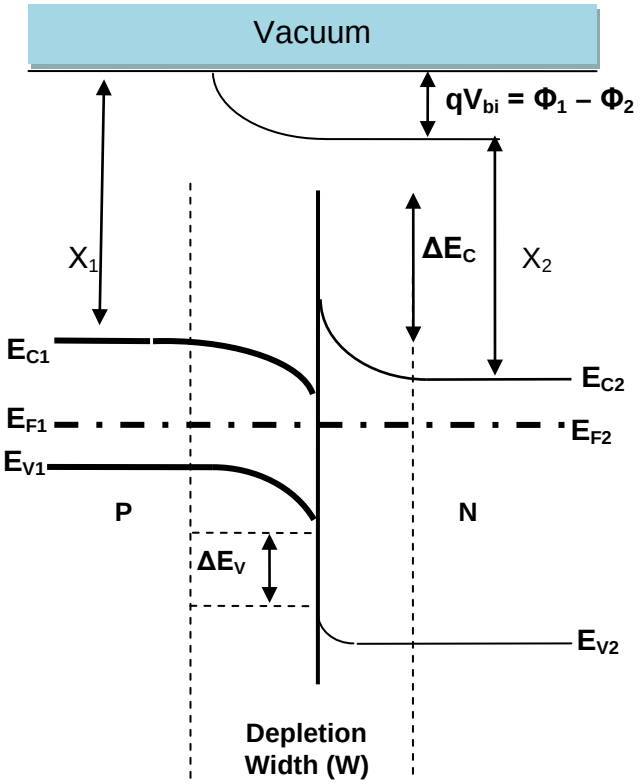

Figure (1.4), P and N type material energy band diagram after junction formation.

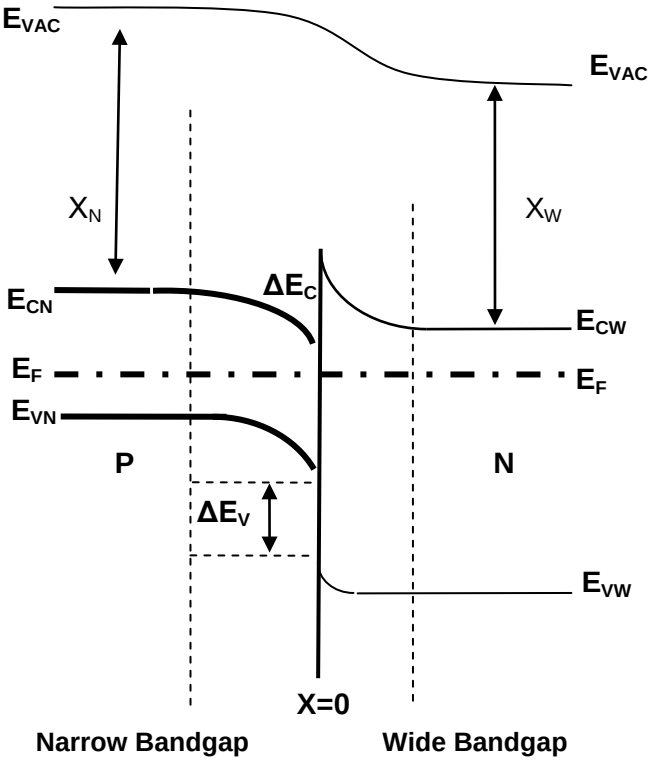

Figure (1.5), Anisotype Semiconductor Heterojunction

E_{VN} – Valence band energy of narrow bandgap semiconductor.
E_{CN} – Conduction band energy of narrow bandgap semiconductor.
E_{VAC} – Vacuum energy level.
E_F – Fermi energy level.
X_N **and** X_W – Electron affinity of narrow and wide bandgap semiconductor.

III. DIFFERENT TECHNIQUES USED FOR PREPARATION OF HETEROJUNCTIONS

Different techniques have been used to fabricate heterojunction device using thin films of II-VI and III-V semiconductors over Silicon, some of the noticeable techniques have been described here. The thin films are generally prepared by chemical spray pyrolysis, vacuum thermal evaporation, chemical bath deposition method (**CBD**), Epitaxial growth from vapour phase, alloying technique and Microreactor-Assisted Solution Deposition (MASD™).

3.1 Vacuum Thermal evaporation technique.

The vacuum thermal evaporation deposition technique consists in heating until evaporation of the material to be deposited. The material vapour finally condenses in form of thin film on the cold substrate surface and on the vacuum chamber walls. Usually low pressures are used, about 10^{-6} or 10^{-5} Torr, to avoid reaction between the vapour and atmosphere. At these low pressures, the mean free path of vapour atoms is the same order as the vacuum chamber dimensions, so these particles travel in straight lines from the evaporation source towards the substrate. A resistance-heated evaporation source is relatively simple and inexpensive, but the material capacity is very small. coiled filaments are typically three stranded tungsten wires looped into coils. Multi-strand filaments are generally used because they offer a greater surface area than single wire filaments.

Under these conditions, the evaporant charge should be small compared with the mass of the filament. The filament can hold up to 1g of evaporant material, formed into staple-like shapes and hung on the central helix of the tungsten filament. Upon melting, the evaporant wets to the filament and is held in place by surface tension. Spreading of the molten evaporant across the wire is desirable to increase evaporation surface area. This is accomplished by distributing the initial charge evenly over the entire length of the filament coil. To minimize dripping of the molten material, the filament coil temperature must be increased rapidly to between 1200°C and 1500°C. Using this technique, the molten material will climb or cling to the hot wire and vaporize efficiently.

Another type of element coil is the filament basket, used to evaporate pellets or chips of materials which either sublime or do not wet the filament wire upon melting. If wetting occurs, the coils of the basket are shorted and the temperature of the source drops. Metal foil boat type resistive elements are yet another choice for small evaporation applications. Metal foil boats are made from thin refractory metal stampings, usually tungsten, molybdenum or tantalum. These boats have dimples which hold the evaporation material. Their miniature size and small capacity make them ideal for small evaporation jobs. Metal foil boats operate at very high temperatures and may cause alloying to occur with certain types of evaporation materials. Wetting of the metal surface by the molten evaporant is desirable in the interest of good thermal contact; however, the molten metal will lower the electrical resistance of the foil in the melt area, thereby causing a drop in temperature. This problem can be eliminated by using a boat which has been coated with a thin layer of aluminum oxide. The oxide coating will not allow wetting of the molten metal evaporant to the metal foil element.

Crucible heaters are an open, circular wound filament which allows crucibles to be inserted inside the windings. The crucibles are commonly manufactured from alumina, carbon, quartz and boron nitride. Crucibles have insulating properties which form a thermal barrier between the filament and melt, allowing a uniform melt temperature. Crucible evaporation is very stable because of its uniform heating. A wide range of low to moderate temperature metals like palladium, tin, selenium, arsenic, indium and organic materials evaporate well from crucibles. Crucibles are less prone to failure compared to metal foil boats because of the complete isolation between the evaporant and the heater element, thus eliminating shorting or alloying. The construction of the resistive heating evaporation chamber along with internal diagrams have been shown in the figure (1.6)a, (1.6)b, (1.6)c and (1.6)d.

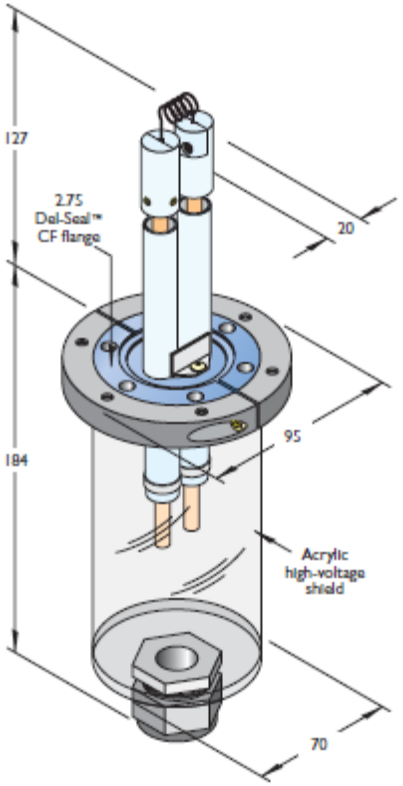

Figure (1.6)a, Resistive heater source assembly.

Figure (1.6)b, Coated metal foil boat.

Figure (1.6)c, Filament coil

Figure (1.6)d, Oxide crucible

Oxide layers on single crystal Silicon wafer are often formed and to get rid of it, the sample is immersed in 10% of HF for 3 to 4 mins. Electrical resistivity lying between 1 to 5 ohms thin film was deposited on Silicon wafer at substrate temperature of 100°C by thermal resistive technique. A 20nm thick layer of Indium film was deposited on the thin film layer at a thermal diffusion temperature of ($\mathbf{T_d}$) ranging between 200 to 300°C was conducted in a vacuum tube furnace [1].

3.2 Spray pyrolysis

Spray pyrolysis is a process in which a thin film is deposited by spraying a solution on a heated surface, where the constituent reacts to form a chemical compound. The chemical reactants are selected such that products other than the desired compound are volatile at the temperature of deposition.

In chemical spray pyrolysis, when a droplet of the spray solution reaches the hot substrate, owing to the pyrolytic decomposition of the solution, thin films well adhered to the surface are deposited. The chemical spray pyrolysis (CSP) technique offers an extremely easy way to prepare films with dopants, virtually any element in any proportion by merely adding it in a spray solution. The deposition rate and thickness of the film can easily be controlled for a wide range. It also offers an opportunity to have reactions at low temperatures (100-5000C). Thin films can be deposited on substrates that are less robust materials and on large surfaces. Various parameters including effect of precursors, dopants, substrates temperature, in-situ annealing treatments, and solution concentrations and so on can easily be controlled. Spray pyrolysis instrument with such features has been reported by Golbole, Badera, Shrivastava and Ganesan [3].

CdS films can be deposited on p-type silicon using spray pyrolysis technique [2]. The technique involves 1:1 mixture (by volume) of solutions containing Cadmium Chloride which acts as source of Cadmium ions and thiourea (NH_2)CS as a source of Sulphur ions. Substrate temperature was maintained at 400˚C (with in ± 2˚C). A thin film of Indium was also deposited over the surface of CdS by electron beam evaporation in a vacuum of pressure 1.33 X 10^{-4} Pa. Deposition of Indium film was controlled by deposition controllers (Inficon Leybold). Thermal diffusion of Indium into CdS was carried out at different temperatures ranging between 350˚C to 550˚C by the process of thermal annealing in vacuum of 1.33X10^{-4} pa for around 15 to 30 minutes.

3.3 Chemical bath Deposition (CBD)

Chemical bath deposition (CBD) is a simple and low-cost method that produces uniform, adherent, and reproducible large area thin films. Chemical bath deposition (CBD) is a convenient and low cost technique for growing thin films of many types of materials and is often used to grow the CdS window layer for thin film solar cells. To deposit thin film of CdS using chemical bath deposition technique a chemical bath is used containing 25ml of stirred deionized water, ($CdCl_2$) (2.5ml, 0.12Mole), NH_4Cl (10ml, 0.20Mole), NH_3 (15.0ml, 2.00Mole) [4]. The bath temperature was maintained at 80˚C in a constant temperature water bath under constant stirring during deposition. The substrate was held by a substrate holder and partially immersed in the solution. The entire system was firmly closed using rubber seal. Thiourea solution (2.50ml, 0.60Mol) was added to the solution in the chemical bath. The total solution volume is 55ml with pH around 10.3. The deposition time was around 30 minutes. During deposition the solutions turns from pale yellow to yellow and

finally bright orange. After deposition is finally cleaned using distilled water dried with N_2 atmosphere.

Using CBD thin film deposition of ZnO using six different complexing agents, namely ammonia, hydrazine, ethanolamine, methylamine, triethanolamine and dimethylamine, has been reported [13]. Antimony sulfide and antimony Selenide thin films were deposited by chemical bath method [14].

Beryllium Sulphide (BeS) thin films on glass slide using chemical bath deposition technique were prepared. Characterization of the deposited thin film was carried out using Fourier transforms infrared (FTIR) spectroscopy and spectrophotometers. Thickness of the film in the range between 0.068 and 0.095mm with energy band gap between 2.30 and 4.40eV has been reported [15].

3.4 Epitaxial Growth from Vapour Phase

The technique involves one of the semiconductors in the vapour phase to condense on a crystalline substrate. The substrate controls the orientation of the layer and the layer is termed epitaxial. This allows layers to be doped to any level with highest precision. This technique is widely used to for producing heterojunction based on elemental semiconductors or III-V compounds.

3.5 Alloying technique

An alloyed heterojunction may be produced either by melting all the lower melting point material or by melting only the interface between the materials. The electrical properties show no dependence on the way of fabrication. The fabrication technique is very simple.

3.6 Microreactor-Assisted Solution Deposition (MASD^{TM})

It consists of flow system and a microscale T-mixer and adjustable residence time microchannel heat exchanger. The CdS film was deposited by the mixture of two streams A and B of reagents. Stream A consisted of Cadmium Chloride (0.004M), ammonium Chloride (0.04M) and Ammonium hydroxide (0.04M) in water. Stream B consisted of Thiourea (0.08) in water. Reagents from the two streams are mixed in T-Mixer before entering the heat exchanger. The substrate is placed on a heater where the temperature is maintained at the deposition temperature. Several combinations of temperature, residence time and deposition time were investigated [5].

3.7 Sintering

Sintering is a method used to create films, layers or objects from powders. The principle of Sintering is based on atomic diffusion. Diffusion is observed in any material when the temperature is above absolute zero, but it occurs much faster as the sample temperature is increased. The powdered material is held in a mould and then heated to a temperature below the melting point. The atoms in the powder particles diffuse across the boundaries of the particles, fusing the particles together and creating one solid piece of layer. Sintering is often chosen as the shaping process for materials with extremely high melting-points such as tungsten and molybdenum as the sintering temperature does not have to reach the melting point of the material. Sintering was traditionally used for manufacturing ceramic objects, but finds applications in almost every field of industry. The study of sintering and of powder-related processes is known as powder metallurgy. CdS films can be prepared by screen-printing followed by sintering process. CdS powder is very well commercially available with 99.99% purity and it can be used as the starting material for the thin film production. CdS powder, 10% wt. of $CdCl_2$ and an appropriate amount of ethylene glycol are thoroughly mixed. $CdCl_2$ can be used as an adhesive and ethylene glycol as a binder. Glass substrates are ultra cleaned by embry powder and acetone and after than a final wash is carried out using high purity distilled water. The paste of CdS powder along with $CdCl_2$ and ethylene glycol was screen printed on ultra clean glass substrates. The sample was dried in open air at 120˚C for four hours. Samples are dried in lower temperature to avoid cracks. Removal of organic materials take place at 400˚C and the temperature for sintering is also maintained at 400˚C. The melting point of Cadmium chloride is 568˚C and it is hygroscopic in nature. The evaporation of CdCl2 starts around 400˚C and it is also to note that to get a stable CdS sintered film $CdCl_2$ and organic material cannot reside together. It was reported that $CdCl_2$ in CdS films enhances the sintering of CdS films [6] meaning that $CdCl_2$ served as a flux to promote particles fusion and granule re-growth at relatively low temperature and finally evaporated during sintering. The sintering temperature ranging between 620˚C and 650˚C was very optimum for sintering of CdS films with $CdCl_2$ in nitrogen atmosphere [7].

IV. Experimental Instruments, Measurements and Observations

Instruments used for structural Analysis of heterojunctions.

There have been several techniques which can confirm that a heterojunction have an ordered structure and that its properties are due only to the interface between the two semiconductors.

4.1 Scanning Electron Microscopy

The structural and morphological analysis of any thin film like CdS, CdTe can be carried out using **Scanning Electron Microscopy** (SEM). The scanning electron microscope (SEM) uses a focused beam of high-energy electrons to generate a variety of signals at the surface of solid specimens. The signals that derive from electron-sample interactions reveal information about the sample including external morphology (texture), chemical composition, and crystalline structure and orientation of materials making up the sample. Accelerated electrons in an SEM carry significant amounts of kinetic energy, and this energy is dissipated as a variety of signals produced by electron-sample interactions when the incident electrons are decelerated in the solid sample. These signals include secondary electrons (that produce SEM images), backscattered electrons (BSE), diffracted backscattered electrons (EBSD that are used to determine crystal structures

and orientations of minerals), photons (characteristic X-rays that are used for elemental analysis and continuum X-rays), visible light (cathodoluminescence--CL), and heat. Secondary electrons and backscattered electrons are commonly used for imaging samples: secondary electrons are most valuable for showing morphology and topography on samples and backscattered electrons are most valuable for illustrating contrasts in composition in multiphase samples (i.e. for rapid phase discrimination). X-ray generation is produced by inelastic collisions of the incident electrons with electrons in discrete orbital's (shells) of atoms in the sample. As the excited electrons return to lower energy states, they yield X-rays that are of a fixed wavelength (that is related to the difference in energy levels of electrons in different shells for a given element). Thus, characteristic X-rays are produced for each element in a mineral that is "excited" by the electron beam. SEM analysis is considered to be "non-destructive"; that is, x-rays generated by electron interactions do not lead to volume loss of the sample, so it is possible to analyse the same materials repeatedly.

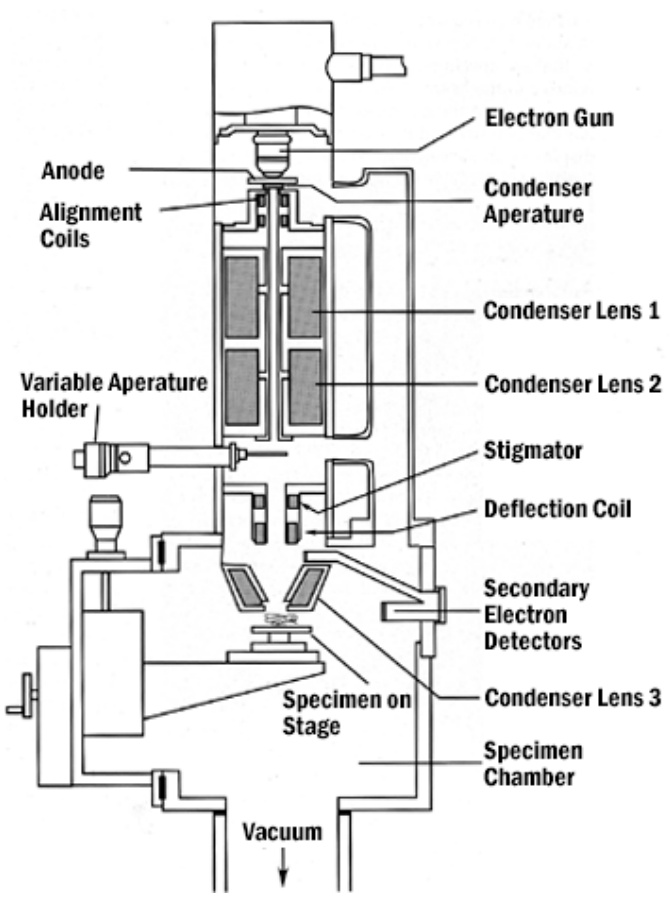

Figure (1.7), Scanning Electron microscope

4.2 Scanning Tunnelling Microscope

The **scanning tunnelling microscope** (STM) is a type of electron microscope that shows three-dimensional images of a sample. In the STM, the structure of a surface is studied using a stylus that scans the surface at a fixed distance from it. An extremely fine conducting probe is held close to the sample. Electrons tunnel between the surface and the stylus, producing an electrical signal. The stylus is extremely sharp, the tip being formed by one single atom. It slowly scans across the surface at a distance of only an atom's diameter. The stylus is raised and lowered in order to keep the signal constant and maintain the distance. This enables it to follow even the smallest details of the surface it is scanning. Recording the vertical movement of the stylus makes it possible to study the structure of the surface atom by atom. A profile of the surface is created, and from that a computer-generated contour map of the surface is produced. The study of surfaces is an important part of physics, with particular applications in semiconductor physics and microelectronics. In chemistry, surface reactions also play an important part, for example in catalysis. The STM works best with conducting materials, but it is also possible to fix organic molecules on a surface and study their structures. For example, this technique has been used in the study of DNA molecules.

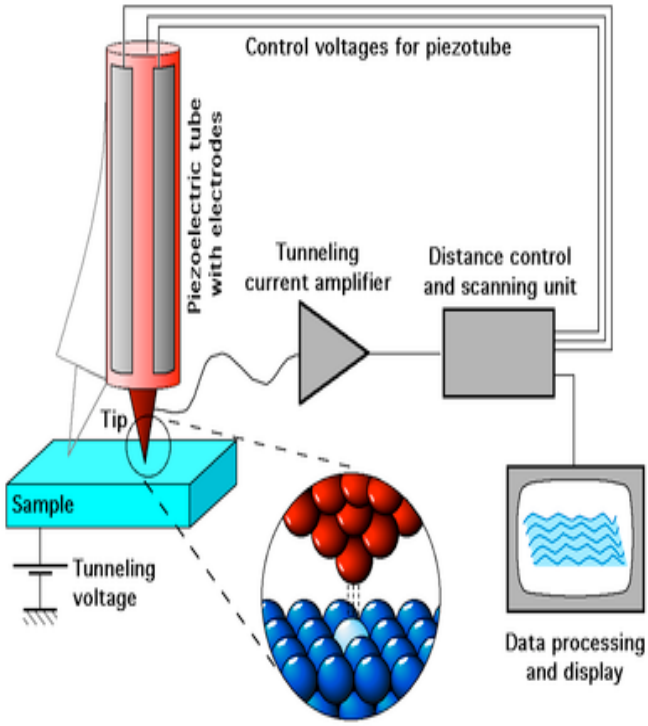

Figure (1.8), Scanning tunnelling microscope

4.3 Atomic Force Microscope

The **Atomic Force Microscope** was developed to overcome a basic drawback with STM - that it can only image conducting or semiconducting surfaces. The AFM, however, has the advantage of imaging almost any type of surface, including polymers, ceramics, composites, glass, and biological samples. The atomic force microscope (AFM) was also invented by Binning et al. in 1986. The AFM measures the forces acting between a fine tip and a sample. The tip is attached to the free end of a cantilever and is brought very close to a surface. Attractive or repulsive forces resulting from interactions between the tip and the surface will cause a positive or

negative bending of the cantilever. The working has been shown in the figure (1.9) and figure (1.10).

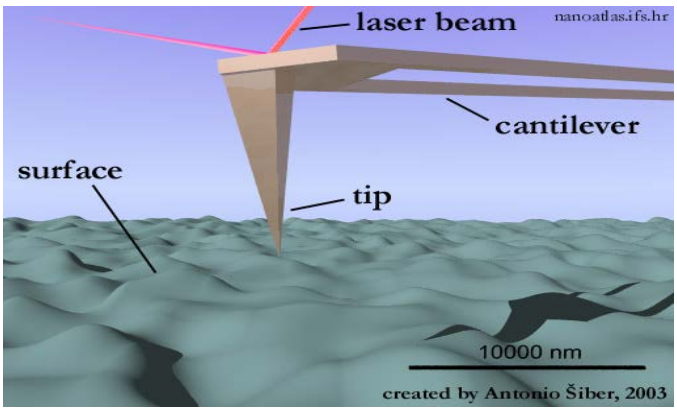

Figure (1.9), Atomic force microscope

The bending is detected by means of a laser beam, which is reflected from the cantilever.

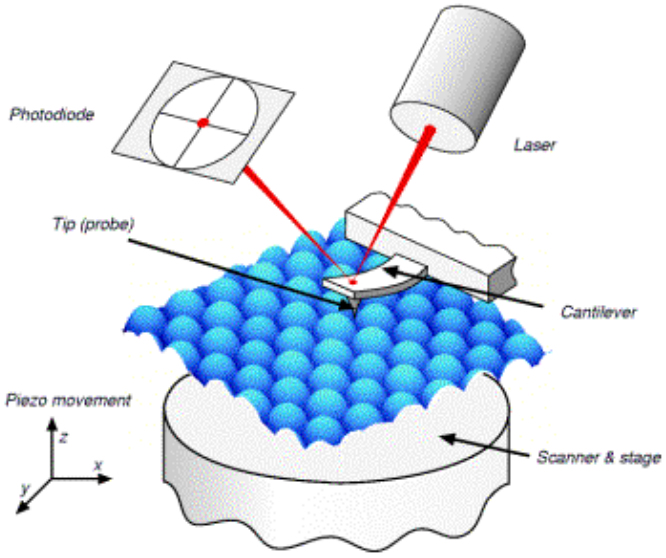

Figure (1.10), Scanning tunnelling microscope

AFM provides a number of advantages over conventional microscopy techniques. AFMs probe the sample and make measurements in three dimensions, *x*, *y*, and *z* (normal to the sample surface), thus enabling the presentation of three-dimensional images of a sample surface. This provides a great advantage over any microscope available previously.

band structure of the junction. Various forms of heterojunctions have been studied extensively for past many years. In this review report stress has been given on the various heterojunctions based on III-V, II-VI semiconductors over silicon and Germanium. There is an effort to summarize the various works done on the heterojunctions. The current density and voltage properties of CdS/Si and CdS:In/Si heterojunctions measured in dark condition under both forward as well as reverse condition yields rectification characteristics and shows strong dependence on Indium diffusion temperature. Indium diffusion shows a significant effect on the reverse breakdown of heterojunction based on CdS/Si, it increases to 10-15 Volts, whereas only CdS/Si without indium shows soft breakdown of 2Volts. The ideality factor is found to be around 3.3 for CdS/Si and 2 for CdS:In/Si at T_d = 300˚C. This also shows that CdS/Si doped with Indium shows better diode characteristics than without [1]. It is also observed that the built in potential decreases with diffusion temperature but it is also observed that if the diffusion temperature increases to 350˚C the built in potential increases. The built in potential is found to be maximum for CdS/Si without Indium diffusion. The doped photodetector that prepared with T_d = 300˚C exhibits the best junction quality. Cadmium sulfide (CdS) thin films are commonly used as buffer layers in thin film solar cells and can be prepared using MASD technology. CdS is deposited on fluorine-doped tin oxide (FTO) coated glass substrate using MASD [5]. A layer of 69nm thick CdS over a 3.7µm thick FTO layer is studied for electrical properties. Dark and illuminated condition current-voltage characteristics has been studied and it has been observed that dark current from 2.1 X 10^{-7} increases to 1.2 X 10^{-5} under illuminated condition, indicating the generation of photocurrent carriers. The electrical property has been shown in figure (1.11) as reported [5].

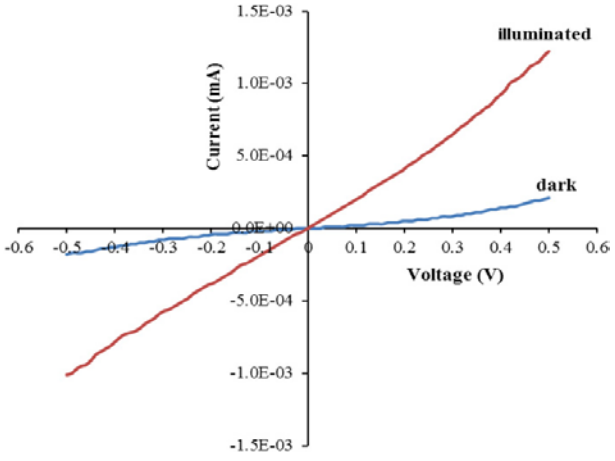

Figure (1.11), V-I characteristic of CdS over FTO under illuminated and dark conditions.

Experimental Observations

4.4 Current-Voltage Characteristics

Standard current-voltage measurements enable the built-in potential to be found and thus can yield information on the

Heterojunction solar cells based on CdS:In/Si fabricated by the process of electron beam evaporation of CdS, have been extensively studied. The electrical and photovoltaic properties have been studied. The I-V characteristics of the heterojunction solar cell shows good agreement with the tunnelling model [8]. To obtain optimum fabrication different

parameters were changed like doping concentration, substrate temperature and annealing temperature under various ambient like H_2, N_2 and Sulphur vapours.

It was also reported that the solar cell fabricated by CdS:In/Si shows no degradation even after 30 months in open air but CdS:In:Ag/Si showed significant degradation in three months. Typical dark forward current (I) versus voltage (V) characteristics for n-CdS/p-Si cell treated under N2 ambient at 350˚C for 5 minutes shows maximum current with less forward voltage drop at temperature 303K and the similar current is obtained but with greater forward voltage at temperature of 101K. This can be seen in the figure (1.12)a. The temperature dependence of the fabricated solar cell was recorded for open circuit voltage and output shorted circuited current has been shown in the figure (1.12)b.

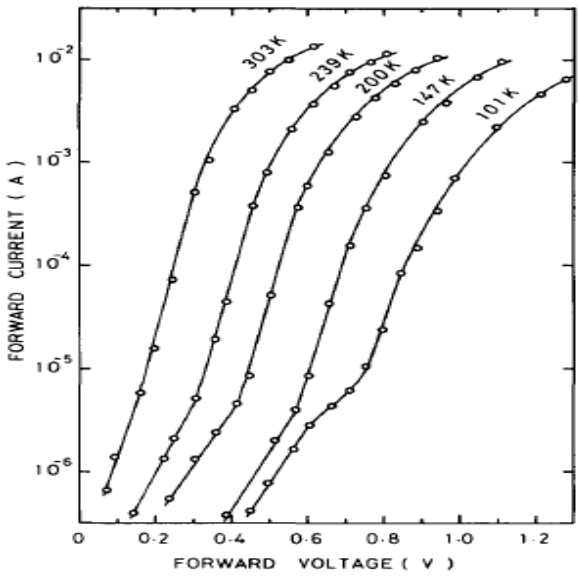

Figure (1.12)a, Typical dark current (I) versus voltage (V) characteristics of an n-CdS/p-Si cell heat treated in N2 ambient at 350˚C for 5 minutes.

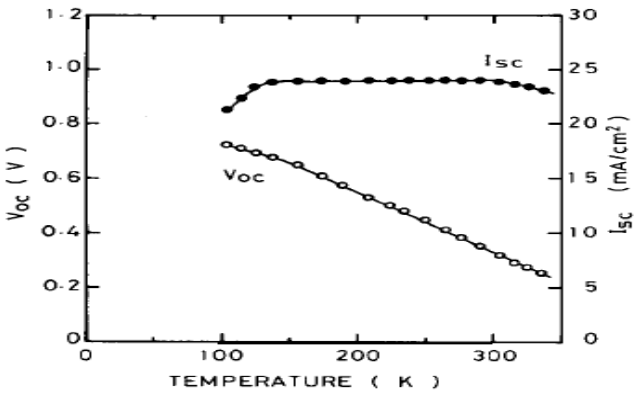

Figure (1.12)b, the temperature dependence of the fabricated solar cell was recorded for open circuit voltage (V_{OC}) and output shorted circuited current(I_{SC}).

With recent developments in nanotechnology, p–n heterojunctions based on semiconductor nanostructures have affected the industry in better way and have shown unique optical and electrical properties. As compared with the film or bulk counterparts, the nanoscale p–n heterojunctions possess superior performances in terms of atomically sharp interfaces, fewer interface defects, and higher emitting efficiency. Intrinsic CdS nanorods (NRs) are highly insulating and thus not suitable for nano-optoelectronic applications. Therefore, gallium doped n-type CdS NRs instead of intrinsic ones were used to fabricate the heterojunction device. Heterojunction, a host of high-performance nano-optoelectronic devices, including nano-LEDs, nano-photodetectors, and nano-PV devices were realised. ***I–V*** characteristics of the CdS NR/Si heterojunction measured in the dark, revealing an excellent rectification characteristic of the heterojunction with a rectification ratio up to 10^4 within ±1.5V. Rectification curve, a low turn-on voltage of 0.8 V can be deduced at the forward bias direction. For an ideal diode, the rectification curve can be expressed using the following equation:

$$I_{DS} = I_0(e^{V_{DS}/nK_BT} - 1). \quad \text{..... (1)}$$

From equation (1), the ideality factor *n* can be written as

$$n = \frac{q}{K_B T}\frac{dV}{d\ln I} \quad \text{..... (2)}$$

Where, I_0 is the reverse bias leakage current, K_B and T are the Boltzmann constant and the temperature in Kelvin, respectively. According to the Sah–Noyce–Shockley theory, *n* is a function of the bias voltage, and the value for *n* is typically equal to 1.0 at a low voltage and 2.0 at a higher voltage for a p–n junction. Here, by fitting the rectification curve following equation (2) (figure 1.13), we obtain n = 0.95 in the low-bias zone (0–0.1 V) and n = 2.4 in the high bias zone (0.1–0.5 V), which is in good agreement with the theoretical values [9].

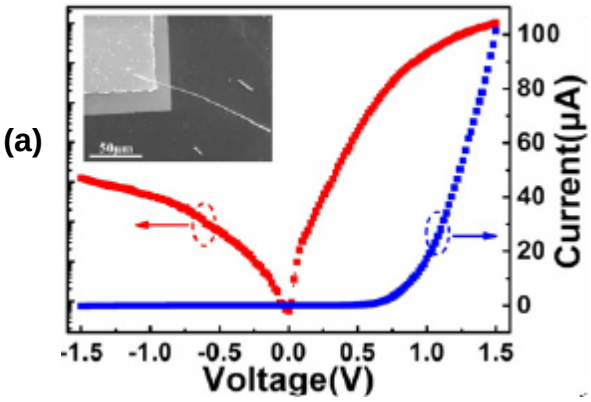

Figure (1.13)a, the V-I characteristics of CdS:Ga NR and Si heterojunction,

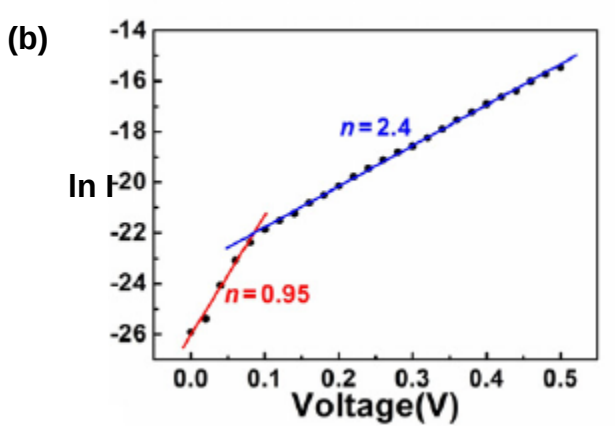

figure(1.13)b, Voltage versus log of device current for measuring the ideality factor.

The ideality factor at high bias is larger than the theoretical value (n = 2.0), maybe due to the Ohmic contact between metal and semiconductor at a low bias and a high bias. In addition, the lattice mismatch between the CdS NR and Si interface leads to a high defect density, a reduction of carrier mobility and an increased equivalent series resistance, which are also responsible for the larger ideality factor. The excellent rectification characteristic shows that high-quality CdS NR/Si heterojunctions were fabricated. The V-I characteristics under dark and illuminated condition has been shown in the figure (1.14).

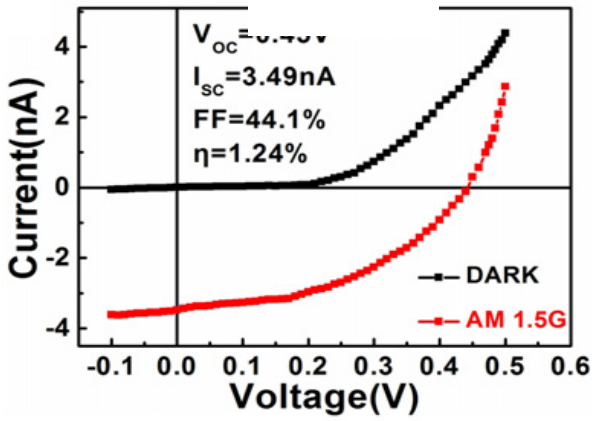

Figure (1.14), the V-I characteristics of CdS:Ga NR and Si heterojunction under illuminated and dark condition.

CdS:Ga NR /Si can be used as nanoLED as shown in the figure (1.15)a, at forward +1.5V, a bright light with yellow colour was observed. Reverse process is also seem viable as the I-V curves both at illuminated and dark show promising effects of possible candidate of a PV cell [9] as shown in the figure (1.15)b. Compared to silicon PV cells CdS:Ga NR/Si shows wider absorption of light spectrum but silicon PV cells show poor response in shorter wavelengths.

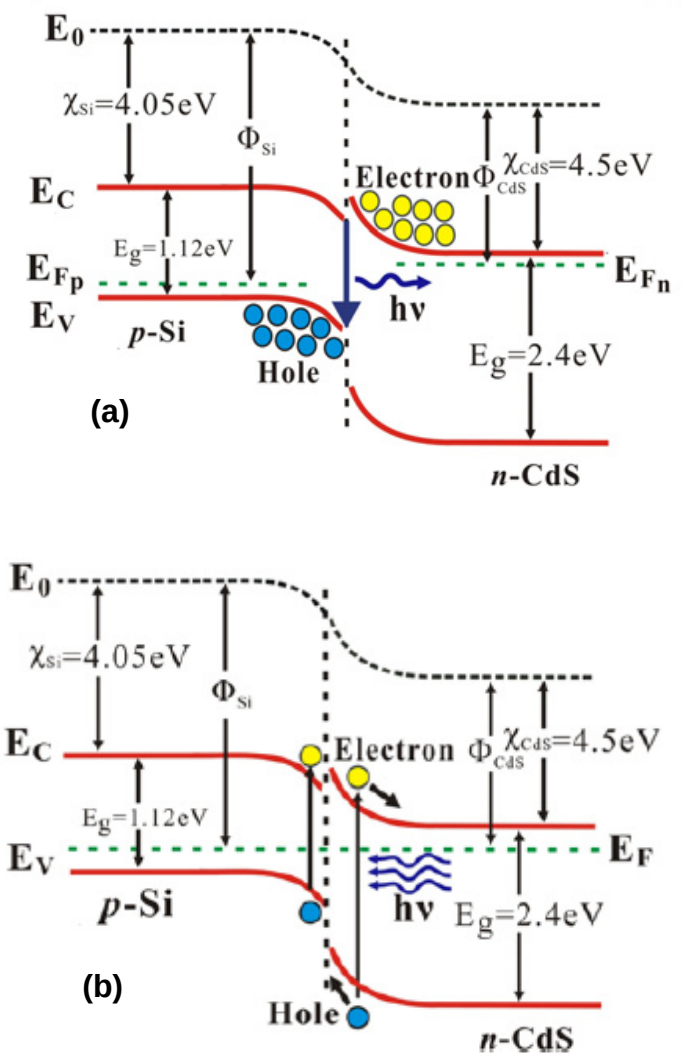

Figure (1.15)a, Energy band diagram of the CdS NR/Si LED under the forward bias, figure (1.15)b, Energy band diagram of the CdS NR/Si PV device under illumination.

PV behavior could be observed for the device, and the open circuit photo voltage (V_{OC}) and the short circuit current (I_{SC}) are deduced to be 0.45 V and 3.49nA, respectively, leading to a fill factor (FF) of 44.1% and a power conversion efficiency (η) of 1.24%.

PV cell constructed out of CdS/p-Si:H shows sensitivity to blue range of electromagnetic spectrum of light [10]. A positive influence has been observed in the photo- response or the optoelectronic properties of the device as the CdS/Si:H exhibits photocurrent in the blue and green region.

n-CdS/p-InP heterojunction showed efficiency of 12.6%. The I-V characteristics were studied for dark conditions with varying temperature. It has been established that the charge transport mechanism is due to tunneling or by recombination in charge depleted region [12].

Lead Sulphide thin films have been deposited on amorphous and fluorine doped tin oxide (FTO) coated glass substrates using simple and inexpensive chemical bath deposition technique. The PbS thin films were grown on an amorphous and FTO-coated glass substrates and various characteristics have been studied. The I-V characteristics of the deposited thin film over FTO have been studied under ± 1V. As the

forward voltage is increased the forward current seems to be increasing exponentially. I-V characteristics in the dark and under light illumination has been shown figure (1.16).

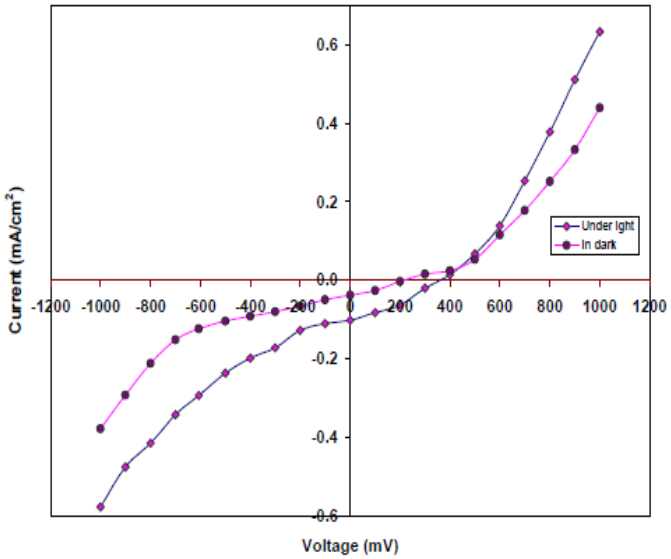

Figure (1.16), the V-I characteristics of chemically deposited PbS thin films.

Such phenomenon can be attributed to tunneling mechanism and small contact heights [16].

4.5 Junction Capacitance measurements

Anderson, Hamphire and Wright have used a modified homojunction theory to predict the value of capacitance for heterojunction, assuming that the doping of the semiconductor is constant up to interface. If the junction is not abrupt then the value of the built in potential obtained will disagree with the value from the capacitance-voltage measurements [17]. Further information about trapping levels may be obtained by the C-V measurements when both frequency and temperature is varied.

The capacitance-voltage characteristics of an anisotype heterojunction have been reported considering the presence of interface states and series resistance [17]. The evaluation was based on the dependence of the above characteristics on the interface state density, doping concentration, temperature and series resistance. It is shown that the functional dependence of the device capacitance is generally determined by the surface potentials on the two sides of the junction. There have been several models proposed the relation between capacitance and diffusion potential [18], frequency and other system parameters [19]. There were limitations in those models, those models did not include the proper description of interface state and series resistance effect. Tersoff [20-22] suggested the concept of midgap energy. The measurement of capacitance require primarily the voltage behavior of surface potentials that may be determined by considering the space charge densities of the two sides of the heterostructures, interface state charge density and charge neutrality condition [23].

4.6 Optical measurements and results

The influence of radiation on the current voltage characteristics of wide bandgap semiconductor has been extensively studied. CdS have been extensively studied and proposed as a window layer for photovoltaic characteristics. Such a work has been reported by Mahdi, Kasem, Hassen, Swadi and Ani [24]. The thin films deposited were of very high transmittance and low reflectance in the wavelength range of 500-900nm, which makes the material an important candidate for solar cell production. The optical transmission edge is sharper when the films were annealed at 200˚C and 300˚C indicating that annealing temperature can improve the crystallinity. In recent studies ternary semiconductors have received considerable attention because of their possible application in Opto-electronic devices like photo sensors. A ternary semiconductor thin film of copper indium diSelenide (CIS) was prepared by chemical bath deposition technique onto glass substrate at 60oC [25]. Optical absorption studies were carried out in the wavelength ranging between 425-1100nm at room temperature.

High-density and single-crystalline CdS NWs (nanowires) were synthesized at 450˚C by chemical vapor transport technique. Owing to the low synthesis temperature, CdS NWs were successfully grown on transparent conducting oxide (TCO)-coated glass substrates. This MEH-PPV–CdS heterojunction reveals noticeably enhanced visible-light absorption and suppressed visible-light emission. Photovoltaic cells fabricated were operated with 1.62% power conversion efficiency [26].

Photodetectors, which can convert the optical signal to an electrical signal, are also vital to the optoelectronic integration. The proper study of response of a photodetector is very essential as it determines how quickly the photodetector responds to the fast varying optical or light signals. Increase in responsivity may increase the bandwidth of light wave communication. Cadmium Sulphide nanoribbons doped with Gallium and deposited on p type silicon has been reported [9]. Certain optoelectronics measurements have yielded non flat response of device in the spectral range between 500-1100nm. Specific detectivity has been reported for a heterojunction device at 800nm. The responsivity value of 0.46A/W is highest at wavelength of 800nm [1]. Heterojunction photo-diodes made from chemical bath deposition technique of CdO on crystalline silicon showed promising spectral response at both infrared and blue regions of the visible spectrum. The simplicity for making these diodes makes them very attractive for their application as a possible substitute of conventional silicon photo-detectors [27]. These diodes require a low reverse voltage (1.5 V) in order to achieve illumination response.

Thin films of ZnO can also be used as thin films which are eventually deposited by thermal decomposition of Zn ($C_5 H_7 O_2$)$_2$ on semiconductor substrate, n-type silicon, p-type InP and also on transparent glass substrate. The obtained ZnO/Si and ZnO/InP heterostructures were investigated for optical properties by spectrophotometry and surface morphology by AFM. The measured values of optoelectrical parameters in the visible spectral range and the lateral photovoltage characteristics demonstrate the possibility of using ZnO/ n-Si

and ZnO/p-InP heterojunctions for photodetection and photovoltaic devices applications [28].

V. HETEROJUNCTION MODELS

5.1 Anderson's Theory

Advent of improved techniques to fabricate thin film deposited heterojunction gave Anderson the first real opportunity to explain the experimental characteristics of Ge-GaAs heterojunctions.
The band gap profiles at the heterojunction were determined not only by the Fermi level but also the electron affinities. The figure (1.17) shows the energy band diagram of n-p heterojunction at equilibrium.

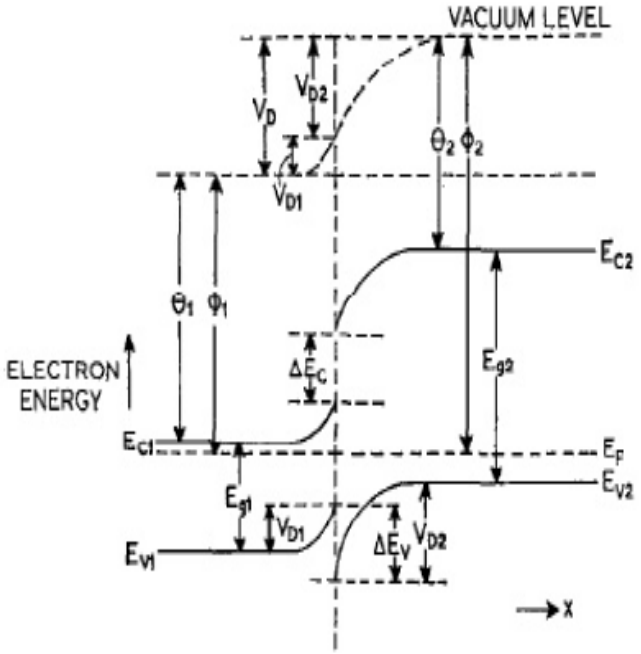

Figure (1.17), energy band diagram of n-p heterojunction at equilibrium.

In the present model the junction was considered to be abrupt with discontinuity at a single line of atom. Shockley's homojunction diffusion theory along with diode emission model was sufficient to predict the saturation current and current-voltage characteristics of Ge-GaAs heterojunction. Anderson's model ignored the effects due to interface states, Lattice misfit between Ge-GaAs is small, giving very few free bonds at the interface.
Anderson indicated that the model may be modified by tunnelling effects, image effects, and carrier generation and recombination. The lowering of potential barrier due to image effect was explained by Hampshire and Wright [29].

5.2 Perlman and Feucht's theory

They propsed a classical, Kinectic, emission model to predict the current-voltage characteristics of an abrupt p-n heterojunction. The effect of electron affinity, electron effective mass, dielectric constants and bad gap at the junction. Anderson completely ignors the effect of spike on the charge carrier trnsport, Perlman and Feucht recognises its decisive role in certain voltage regions. Before being injected the electrons have to pass the spike. This is assumed to take place by thermal emission like in schottky diode with sufficiently long mean free path and its absense of tunnelling. This thermal emission and the subsquent diffussion in the conduction band of the narrow-gap material are two processes in series. If the diffusion is rate dtermining, the I-V characteristics is of the Schokley type. The latter occurs in an anisotype heterojunction for which in equilibrium the top of the spike lies below the conduction band of the narrow-gap material, outside the space charge region. In this case the presense of spike is irrelevent to the low voltage part of the I-V characteristics, which is as predicted by Anderson. The Spike above the bottom of the conduction band of the narrow band gap material, the emission over the spike becomes rate determining.

5.3 Oldham and Milnes Theory

Effect of interface states was first included by Oldham, who considered abrupt heterojunctions with edge dislocations at the interface. Dislocation of 2-4% was assumed to lie in the sheet and to be similar to grain boundaries. They make an assumption that there is a great number of electrically active interface states partially originating from the "dangling bonds" associated with lattice mismatch. These states are probably partly acceptors and partly donors. To reach equilibrium, the materials on both the sides of the interface give off electrons to the acceptors. In the concentration of interface states is high enough, this result in two positively charged depletion layers. The sum of their charges is opposite to and equals the magnitude of the charge of the monopole layer of interface states. The energy band diagram is called the double-depletion layer model. The models have been shown in the figures (1.18)a and b.

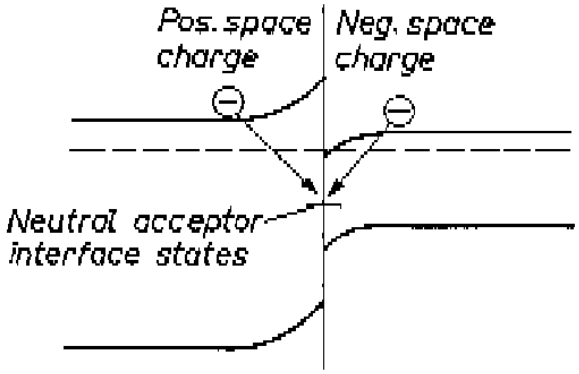

Figure (1.18)a, double depletion layer model before equilibrium with interface states.

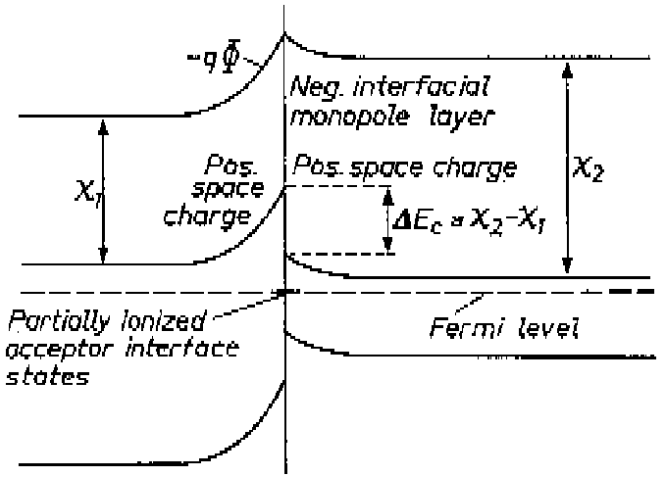

Figure (1.18)b, double depletion layer model after equilibrium has been established.

5.4 Van Ruyven Theory

A more general theory than that of Oldham has been formulated by Van Ruyven. The interface was considered to be similar to two semiconductors, each with a free surface. Interface states were thought to play a decisive role since they can store sufficient charge to make the surface behave like thin, metal layer. Contact between the two different surfaces leads to the formation of dipole layer. Hence the heterojunction consists of three separate junctions; a Schottky barrier between the first semiconductor and its own metal like surface, a metal contact between the planes of surface states containing a dipole, another Schottky barrier between the metal like surface of the second semiconductor itself figure (1.19).

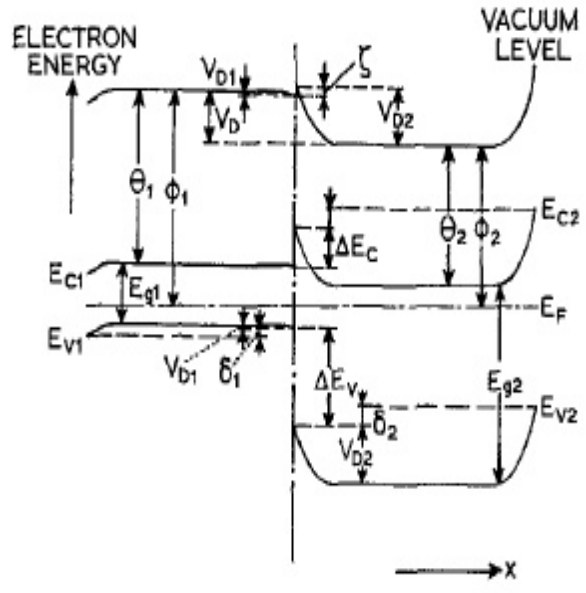

Figure (1.19), Band Profile of a Ge-GaP heterojunction; general case.

This model is the other extreme to that of Anderson model. For sufficiently large interface- state densities, the Fermi level at the interface can be fixed near mid-gap, its position being determined by the work function of the free semiconductor surface and being independent of the Fermi-level position in the bulk. Experiments on the photoelectric effects in Ge-GaP heterojunction provide support for this model.

REFERENCES

[1] Salwan K. J. Al-Ani Raid A. Ismail Hana F.A. Al-Ta'ay, Optoelectronic properties n:CdS:ln/p-Si heterojunction photodetector, Springer 2006.

[2] T.D. Dzhafarov, F. Ongul, S. Aydin Yuksel LÜ WeiFen, "Effect of Indium diffusion on characteristics of CdS films and nCdS/pSi," Elsevier 2010.

[3] Bhavana Godbole, Nitu Badera, S.B. Shrivastav and V. Ganesan,"A simple chemical spray pyrolysis apparatus for thin film preparation", Journal of Instrumentation Society of India, Vol 39-1, 2009.

[4] Sahar Mustafa Asad Khudruj, "CdS thin film photo-Electrochemical electrodes: Combined Electrochemical and chemical bath depositions", An-Najah National University, Faculty of Graduate studies, 2011.

[5] Sudhir Ramprasad, Yu-WeiSu, Chih-hung Chang, Brian K. Paul, Daniel R. Palo "Cadmium sulphide thin film deposition: A parametric study using microreactor-assisted chemical solution deposition", Elsevier, Solar Energy Materials & Solar Cells 96 (2012) 77–85.

[6] D Patidhar, R Sharma, N Jain, T P Sharma and N S Saxena, "Optical properties of CdS sintered film", Indian Academy of Sciences, Vol. 29, No. 1, February 2006, pp. 21–24

[7] V. Kumar1, D. K. Sharma, M.K. Bansal, D.K. Dwivedi, T.P. Sharma, "Synthesis and Characterization of Screen-Printed CdS Films", *Science of Sintering*, **43** (2011) 335-341.

[8] Toshikazu SUDA and Akio KUROYANAGI, "Photovoltaic and electrical properties of n-CdS/p-Si Heterojunction solar cells", Journal of Crystal Growth, North-Holland Publishing Company, 61(1983) 494—498.

[9] DiWu, Yang Jiang, Shanying Li, Fangze Li, Junwei Li, Xinzheng Lan, Yugang Zhang, Chunyan Wu, linbao Luo and Jiansheng Jie, "Construction of high-quality CdS:Ga NR/Silicon Heterojunctions and their nano-optoelectronic applications", Elsevier Nanotechnology **22** (2011) 405201 (6pp).

[10] B. Ullrich, T. Lo¨her b, Y. Segawa a, T. Kobayashi, "The influence of hydrogen passivation of silicon on the photocurrent of CdS:Si heterodiodes" , Elsevier, Materials Science and Engineering B65 (1999) 150–152.

[11] A.A.M. Farag, I.S. Yahiab, M. Fadel, "Electrical and photovoltaic characteristics of Al/n-CdS Schottky dioide", International journal Of Hydrogen energy 34 (2009).

[12] M. Purica, E. Budianu , E. Rusu, P. Arabadji, "Electrical properties of the CdS/InP heterostructures for photovoltaic applications", Elsevier, Thin Solid Films 511 – 512 (2006) 468 – 472.

[13] Hani Khallaf, Guangyu Chai, Oleg Lupan, Helge Heinrich, Sanghoon Park, Alfons Schulte and Lee Chow, " Investigation of CBD of ZnO thin films using six different complexing agents", J. Phys. D: Appl. Phys. **42** (2009) 135304 (8pp).

[14] Y. Rodríguez-Lazcano, L. Guerrero, O.Gomez Daza, M. T. S. Nair,* and P. K. Nair," Antimony Chalcogenide thin films: chemical bath deposition technique and formation of new materials by post deposition thermal process", *Superficies y Vacío* ***9****, 100-103, Diciembre 1999.*
[15] F.I. EZEMA AND C.E. OKEKE, "Chemical Bath deposition of Beryllium Sulphide (BeS) thin film and its application", Academic open internet journal, Vol 9, 2003.
[16] M.A Barote, A.A yadav, T.V Chavan, E.U Masumdar," Characterization and Photoelectrochemical properties of Chemical bath deposited PbS thin films", Digest Journal of Nanomaterials and Biostructures Vol. 6, No 3, July – September 2011, p. 979 – 990.
[17] W. G Oldham and A.G Milnes," Interface states in Abrupt Semiconductors", Sol. State Electron. 7, 153.
[18] R.L. Anderson, Solid State Electron. 5 (1962) 341.
[19] J.P. Donnelly, A.G. Milnes, IEEE. Trans. Electron. Dev. Ed. 14 (1967) 63.
[20] J. Tersoff, Phys. Rev. Lett. 52 (1984) 465.
[21] J. Tersoff, Phys. Rev. B. 30 (1984) 4874.
[22] J. Tersoff, Phys. Rev. B. 32 (1985) 6968.
[23] P. Chattopadhyay, D.P. Haldar, "Capacitance-voltage characteristic of anisotope heterojunction on the presence of interface states and series resistance", Applied Surface Science 171 (2001) 207-212.
[24] M. A. Mahdi, S. J. Kasem, J. J. Hassen, A. A. Swadi, S. K. J.A l-Ani, " Structural and optical properties of chemical deposition CdS thin films", Int. J. Nanoelectronics and Materials **2** (2009) 163-172.
[25] R. H. Bari, L. A. Patil, P. P. Patil, " Studies on Chemically deposited Nonstoichiometric thin films of CuInSe2 a highly promising material for photo sensor" , *Sensors & Transducers Journal, Vol.69, Issue 7, July* **2006,** *pp.629-636.*
[26] Jung-Chul Lee , Wonjoo Lee , Sung-Hwan Han , Tae Geun Kim , Yun-Mo Sung ," Synthesis of hybrid solar cells using CdS nanowires array grown on conductive glass substrates", Electrochemistry Communications 11 (2009) 231–234.
[27] Mauricio Ortega, Guillermo Santana, and Arturo Morales-Acevedo," Optoelectronic property of CdO-Si heterojunctions", *Superficies y Vacío* ***9****, 294-295, Diciembre 1999.*
[28] Munizer Purica, Elena Budianu, Emil Rusu," Heterojunction with ZnO polycrystalline thin films for optoelectronic devices applications", Elsevier, Microelectronic Engineering 51–52 (2000) 425–431.
[29] M.J Hampshire and G.T Wright, "The Si-Ge n-p heterojunctions", Brit J. Appl physics, 15, 1331.

Author: TANMOY BISWAS

Tanmoy Biswas, Assistant Professor in Computer Science, is presently Head of the department and employed by Syamaprasad College, 92, S P Mukherjee Road, Kolkata - 700026 which is affiliated to University of Calcutta. He obtained his graduation (BSc) in Electronics with Honours in the year 1999 and Masters in Electronic Science (MSc) from University of Calcutta in the year 2002 and qualified UGC NET in the year 2005. He also pursued his higher studies in Engineering and obtained Masters in Engineering in the subject Information Technology (ME-IT) from University of Technology (WBUT) in the year 2006. He is also presently attached with West Bengal State University as a Guest Teacher and his area of interest and Teaching includes Analog and Digital Electronics, Analog and Digital Communication, VLSI, Advanced Computer Architecture, Data Communication & Networking and Microprocessors and Microcontrollers.